2 5 8 3 2 2

Application of Spaceborne Scatterometer to Study Typhoon, Tropical Hydrologic Balance, and El Niño

W. Timothy 1.iu

Jet Propulsion Laboratory 300-323
California Institute Of Technology
Pasadena, CA 91109, USA

ABSTRACT

The high spatial resolution and global coverage of a spaceborne microwave scatterometer make it a power instrument to study phenomena ranging from typhoon to El Niño Southern Oscillation which have regional and short term economic and ecological impacts as well as effects on long term and global climate changes. In this report, the application of scatterometer data, by itself, to study the intensity and the evolution of typhoon is demonstrated The potential of combining wind vector and precipitable water derived from two spaceborne sensors to study the hydrologic balance in the tropics is discussed. The role of westerly wind bursts as a precursor of anomalous warming in the equatorial Pacific is investigated with coincident data from microwave scatterometer, altimeter and radiometer.

1. INTRODUCTION

The National Aeronautics and Space Administration Scatterometer (NSCAT) will be launched on the first Japanese Advanced Earth Observing Satellite (ADEOS-1) in August 1996. It will transmit microwave pulses to the Earth's surface and measure the backscattered power which depends on surface roughness. Over ocean, the surface roughness is in equilibrium with the local wind. The main objective of NSCAT is to derive wind speeds and directions over at least 90% of the ice-free global oceans every two days - under both clear and cloudy conditions. The measurements also describe the characteristics of vegetation over land and the movement and morphology of sea ice. The applications are multifaceted and interdisciplinary. In this short report, only a few examples are demonstrated, from using scatterometer alone to synergistic application of an array of spacborne of sensors.

2. TYPHOON

The high spatial resolution (25-50 km) of spacborne scatterometer, unmatched by any numerical weather prediction (NWP) products, makes it a powerful tool to study atmospheric mesoscale systems over data sparse ocean. The use of scatterometer winds to monitor tropical cyclone Oliver was demonstrated as part of the TOGA (Tropical Ocean and Global Atmosphere) COARE (Coupled Ocean Atmosphere Response Experiment) [1,2]. The interpolated wind field from the scatterometer on the European spacecraft ERS 1 (Fig. la) shows in details the circulation around the eye of Oliver at 21 .5°S and 155.5°E, but no cyclone center is obvious in the 2.5° resolution NWP product of the European Center for Medium Range Weather Forecast (ECMWF) in Fig. lb. Atmospheric pressure field is also constructed, using the scatterometer wind alone, through a boundary layer model [3] and gradient wind equation, The pressure field derived from scatterometer data (Fig. 1c) clearly show the intensity of the cyclone not seen the NWP products ECMWF (Fig. id).

In Fig. 2, the surface wind vectors (black arrows) along a ground track of the scatterometer on ERS 1 were overlaid on the gray-scale image representing the precipitable

Liu

258322

water (column integrated water vapor) observed by the Special Sensor Microwave Imager (SSMI). The relation between dynamics and hydrologic balance in the mesoscales is dramatically visualized, as Typhoon Irving approaches Japan. The detailed structure of the wind-field demonstrated the power of the scatterometer. The "all weather" capabilities of microwave sensors makes it possible to observed through clouds. The NASA Scatterometer (NSCAT) scheduled to be launched in 1996 will have twice the coverage as the ERS 1 scatterometer and will provide an unmatched spatial resolution and coverage over the global ocean. The ADEOS-2 spacecraft will include both microwave scatterometer and microwave radiometer it will be launched in 1999 and the coincident measurements will provide good opportunity to study the wind-driven hydrologic balance.

3. TROPICAL HYDROLOGIC BALANCE

The local coupling of atmospheric and oceanic hydrologic balances in the warm pool of western equatorial Pacific is illustrated by a combination of satellite data in Fig, 3 [4]. The precipitable water is derived from SSMI. The surface wind field is derived by combining the wind speed SSMI with all available data through a variational method [5]. Evaporation is computed from wind speed, precipitable water, and sea surface temperature measured by SSMI and the Advanced Very High Resolution Radiometer (AVHRR) [6]. The precipitation is acquired from the GPCP (Global Precipitation Cloud Climatology Project); it is derived from visible and near infrared observations on geostationary satellites [7]. The salinity is measured at a mooring at the equator and 165*E [8]. The climatological annual cycle is removed from each parameter to give the anomalies. The time series show that roughly between early 1988 and late 1989, the anomalies of precipitable water vapor and precipitation are negative while the anomalies of evaporation and salinity are positive, indicating dryer air, higher evaporation and lower precipitation, and a saltier ocean. During this period, the surface wind divergence are positive, indicating convection/convergence is suppressed. Outside of this period, the reverse is true. Convection/convergence is enhanced, the atmosphere has more moisture, evaporation is suppressed, and precipitation is above normal. These changes agree with the decrease in salinity in the ocean. The" figure clearly demonstrates that the hydrologic balance in the atmosphere and the ocean are linked through surface wind divergence; NSCAT will monitor the divergence.

4 . EL NINO

In Fig. 4, three spaceborne sensors were combined to describe a recent warming event (1994- 1995) in the equatorial Pacific [9]. The deviations of the 1994 values of a parameter from its corresponding 1993 values for surface wind stress, sea level, and sea surface temperature are shown and these deviations are, hereafter, referred to as anomalies. In the equatorial eastern Pacific, the Trades Winds generally blow from the west to the east and their zonal components are negative. During the second half of 1994, four distinct groups of equatorial westerly (positive) wind anomalies were observed by the scatterometer on ERS 1 to occur near the date line. Each group of wind anomalies initiated an eastward-propagating, downwelling Kelvin wave that was exhibited as anomalous sea-level rise observed by Topex/Poseidon altimeter. Corresponding to the passage of Kelvin waves are surface-warming episodes observed by AVHRR. The coincident observations infer that the westerly wind anomalies are precursor of El No. The eastward propagation of the anomalous sea level and sea-surface temperature were closely simulated by an Ocean General Circulation Model when it was forced by realistic winds. Model diagnostics, e.g., subsurface temperature field, the currents distribution, and the mixed layer heat budget, are being analyzed to understand the mechanism of wind forced temperature changes during a warming event.

258322

5. CONCLUSION

The spaceborne microwave scatterometer with its high spatial resolution and global coverage is a powerful tool for a wide range of studies. By synergistic combination of the observations by the scatterometer with other sensors on ADEOS 1 and 2, such a, the Advanced Microwave Scanning Radiometer (AMSR) and Ocean Color and Temperature Scanner (OCTS), the global energy-hydrologic cycle and the biogeochemical cycles could be studied There has been operating scatterometer since ERS 1 was launched in 1991 and scatterometers on ERS-2, ENVISAT, ADEOS- 1, and ADEOS-2 will assure more than a decade of continuous ocean surface wind vector observations.

6. ACKNOWLEDGMENTS

This study was performed at the Jet Propulsion Laboratory, California Institute of Technology, under contract with the National Aeronautics and Space Administration (NASA). It was jointly supported by the NASA Earth Observing System, the NASA Scatterometer, and Topex/Poseidon Projects

7. REFERENCES

[1] Liu, W.T., C.S. Hsu, and A. Zhang, "Application of scatterometer winds during TOGA-COARE. TOGA *Notes*, 13,6-7, 1993.

[2] Hsu, C.S. and W.T. Liu, 'Tropical cyclone intensity from scatterometer winds," ***J. Geophys. Res.***, submitted, 1995.

[3] Brown, R. A., and W.T. Liu, "An operational large-scale marine boundary layer model," ***J. Appl. Meteor.; 21, 262-269, 1982.***

[4]Liu, W.T., "Spaceborne scatterometer in synergistic studies of global changes, ***"Environment '93,*** M. Fang and A. Liu (eds.), Commercial Press Ltd., Hong Kong, 284-293, 1993:

[5] Atlas, R., R.N. Hoffman, and S.C. Bloom, "Surface wind velocity over the ocean," ***Atlas of Satellite Observations Related to Global Changes,*** R.J. Gurney, J.L. Foster, and C. L. Parkinson (eds.), Cambridge Univ. Press, London, 129-139, 1993.

[6]Liu, W.T., "Moisture and latent heat flux variabilities in the tropical Pacific derived from satellite data,' ***J. Geophys. Res.,*** 93,6749-6760 and 6965-6968, 1988.

[7] Arkin, P.A., and P.E., Ardanuy, "Estimating climatic-scale precipitation from space: a review," ***J. Climate, 2, 1229-1238.1989.***

[8] McPhaden, M.J., H.P. Freitag, and A.J. Shepherd, "Moored salinity time series measurements at 0°, 140°W," ***J. Atmos. Ocean. Tech., 7,568-575, 1990.***

[9]Liu, W.T., W. Tang, and L.L. Fu, "Episodic wind forcing of a tropical warming event as observed by spaceborne sensors," Eos Transaction of Amer. Geophy. Union, accepted for publication, 1995.

258322

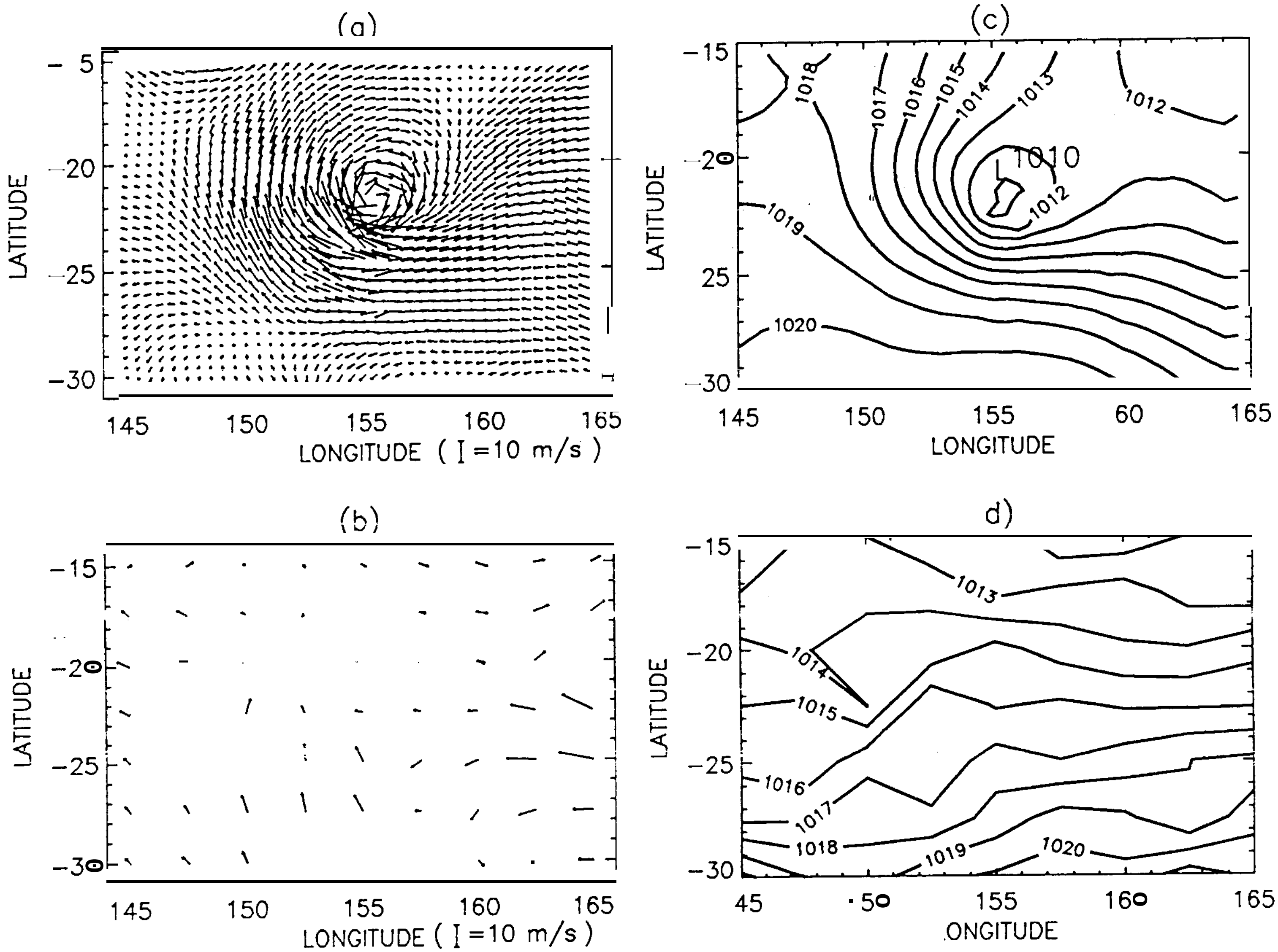

Fig. 1 Surface wind fields derived from ERS1 scatterometer observations (a) and ECMWF numerical weather prediction (b). Surface pressure field derived from ERS1 wind field (c) and from ECMWF (d), at 00 UTC on February 12, 1993, from [1].

2 5 8 3 2 2

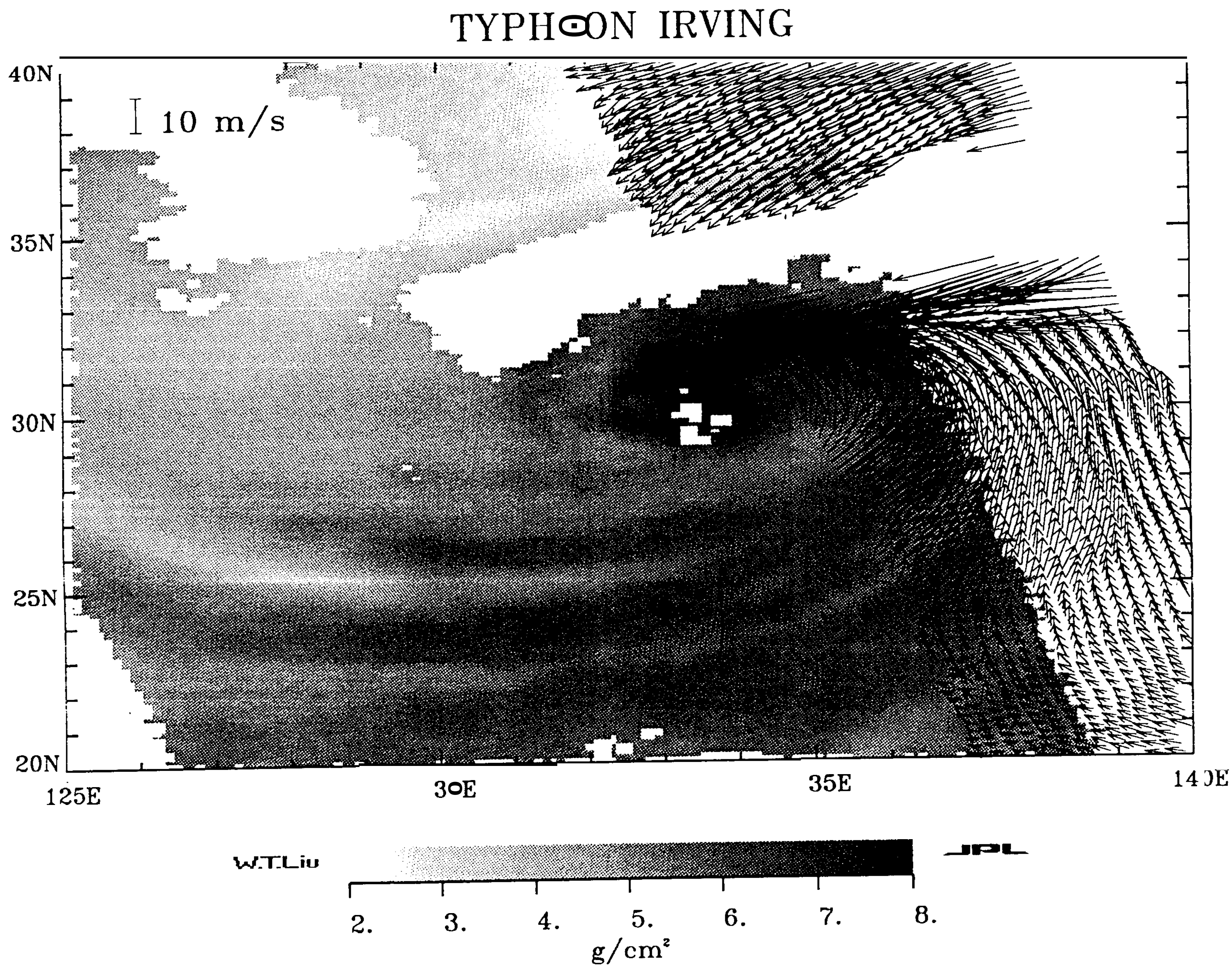

Fig. 2 Typhoon Irving revealed by the wind vectors from ERS1 scatterometer (dark arro and the precipitable water from SSMI (gray scale image) as it hits the Honshu Island of Japan on August 3, 1992.

Liu

57

2 5 8 5 2 2

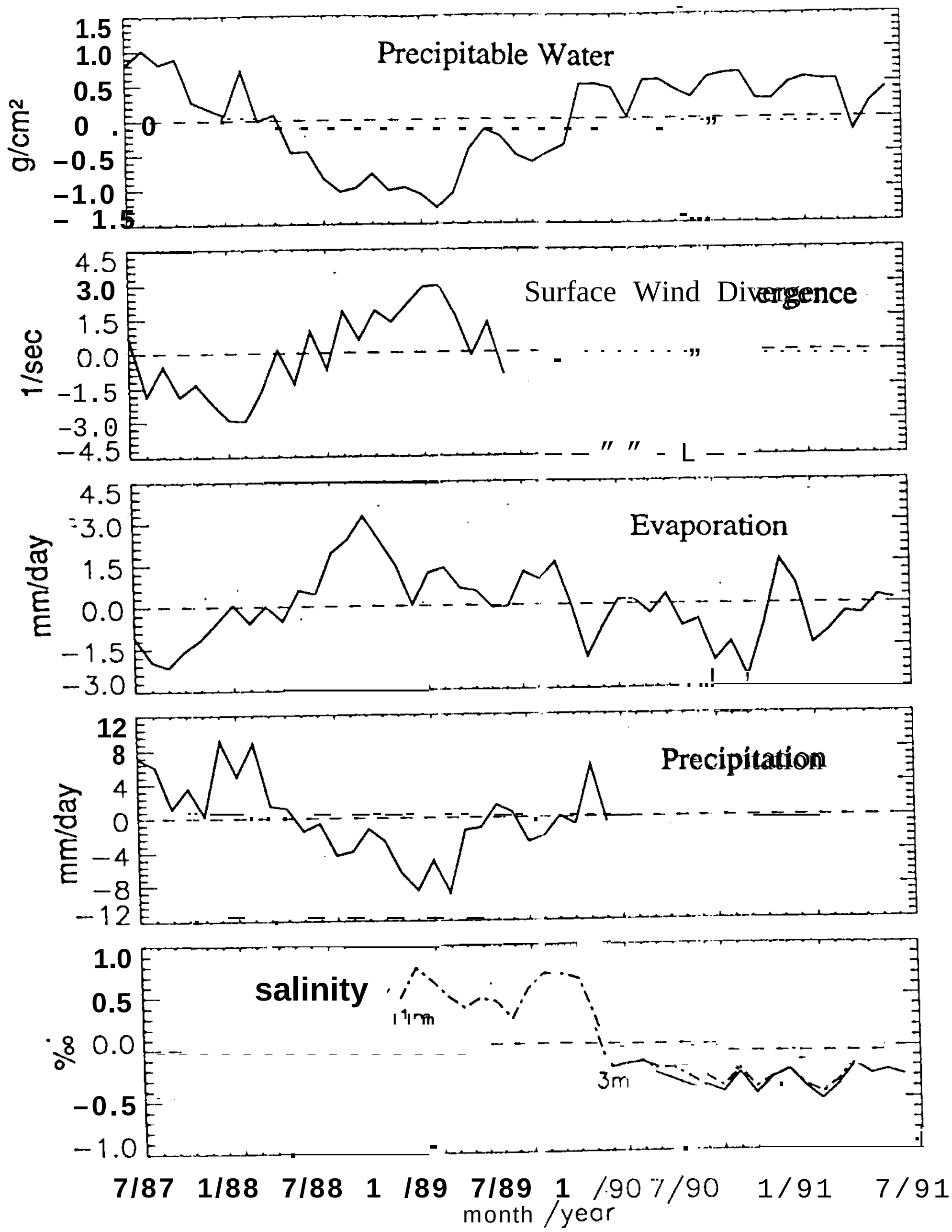

Fig. 3 Anomalous variations of (from top to bottom) precipitable water derived from SSMI, surface wind divergence from a combination of SSMI wind speed and wind direction based on a variational analysis of all available data, evaporation from SSMI and AVHRR, rainfall from the Global Precipitation Climatology Project, and salinity at two surface levels of an equatorial mooring at 165°E on the equator, from [4].

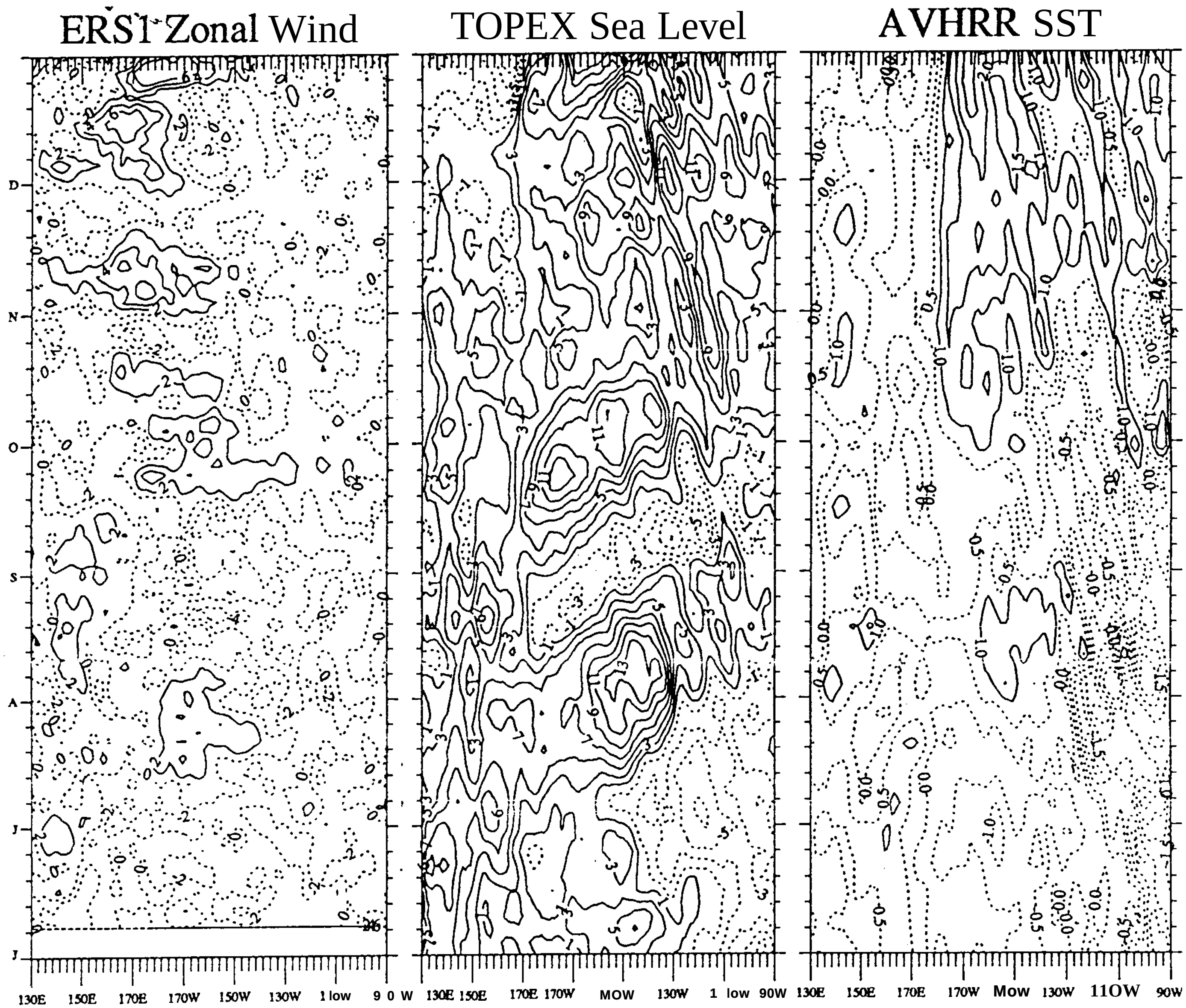

Fig. **4** Time-longitude variations, along the equator, of anomalous zonal wind stress (left), sea level (center), ” and sea surface temperature (right). They are derived from the ERS 1 scatterometer, the Topex/Poseidon altimeter, and the AVHRR blended with in situ measurements, from [9].